

## NSTX plasma operation with a Liquid Lithium Divertor

H.W. Kugel<sup>a,\*</sup>, J.P. Allain<sup>b</sup>, M.G. Bell<sup>a</sup>, R.E. Bell<sup>a</sup>, A. Diallo<sup>a</sup>, R. Ellis<sup>a</sup>, S.P. Gerhardt<sup>a</sup>, B. Heim<sup>b</sup>, M.A. Jaworski<sup>a</sup>, R. Kaita<sup>a</sup>, J. Kallman<sup>a</sup>, S. Kaye<sup>a</sup>, B.P. LeBlanc<sup>a</sup>, R. Maingi<sup>c</sup>, A. McLean<sup>c</sup>, J. Menard<sup>a</sup>, D. Mueller<sup>a</sup>, R. Nygren<sup>d</sup>, M. Ono<sup>a</sup>, S.F. Paul<sup>a</sup>, R. Raman<sup>e</sup>, A.L. Roquemore<sup>a</sup>, S.A. Sabbagh<sup>f</sup>, H. Schneider<sup>a</sup>, C.H. Skinner<sup>a</sup>, V.A. Soukhanovskii<sup>g</sup>, C.N. Taylor<sup>b</sup>, J.R. Timberlake<sup>a</sup>, M. Viola<sup>a</sup>, L. Zakharov<sup>a</sup>, NSTX Research Team

<sup>a</sup> Princeton Plasma Physics Laboratory, Princeton, NJ 08543, USA

<sup>b</sup> Purdue University, West Lafayette, IN 47907, USA

<sup>c</sup> Oak Ridge National Laboratory, Oak Ridge, TN 37831, USA

<sup>d</sup> Sandia National Laboratories, Albuquerque, NM 87185, USA

<sup>e</sup> University of Washington, Seattle, WA 98195, USA

<sup>f</sup> Columbia University, New York, NY 10027, USA

<sup>g</sup> Lawrence Livermore National Laboratory, Livermore, CA 94551, USA

### ARTICLE INFO

#### Article history:

Available online 26 August 2011

#### Keywords:

Lithium  
Lithium divertors  
Lithium plasma facing components  
Lithium impurities  
Divertors

### ABSTRACT

NSTX 2010 experiments were conducted using a molybdenum Liquid Lithium Divertor (LLD) surface installed on the outer part of the lower divertor. This tested the effectiveness of maintaining the deuterium retention properties of a static liquid lithium surface when refreshed by lithium evaporation as an approximation to a flowing liquid lithium surface. The LLD molybdenum front face has a 45% porosity to provide sufficient wetting to spread 37 g of lithium, and to retain it in the presence of magnetic forces. Lithium Evaporators were used to deposit lithium on the LLD surface. At the beginning of discharges, the LLD lithium surface ranged from solid to liquefied depending on the amount of applied and plasma heating. Noteworthy improvements in plasma performance were obtained similar to those obtained previously with lithiated graphite, e.g., ELM-free, quiescent edge, H-modes. During these experiments with the plasma outer strike point on the LLD, the rate of deuterium retention in the LLD, as indicated by the fueling needed to achieve and maintain stable plasma conditions, was the about the same as that for solid lithium coatings on the graphite prior to the installation of the LLD, i.e., about two times that of no-lithium conditions. The role of lithium impurities in this result is discussed. Following the 2010 experimental campaign, inspection of the LLD found mechanical damage to the plate supports, and other hardware resulting from forces following plasma current disruptions. The LLD was removed, upgraded, and reinstalled. A row of molybdenum tiles was installed inboard of the LLD for 2011 experiments with both inner and outer strike points on lithiated molybdenum to allow investigation of lithium plasma facing issues encountered in the first testing of the LLD.

© 2011 Elsevier B.V. All rights reserved.

### 1. Introduction

Since 2008, almost all National Spherical Torus Experiment (NSTX) experiments have made use of two Lithium Evaporators (LITERS) to evaporate lithium onto the lower divertor region, at total rates of 10–70 mg/min for periods of 5–10 min between discharges [1–4]. These evaporators were each loaded with up to 80 g of lithium which was exhausted after about 2 weeks of operation. The empty evaporators were then replaced with reloaded ones. This

cycle was performed repeatedly during each experimental campaign.

Lithium evaporated on plasma facing components (PFCs) has the potential for control of density through its ability to absorb the atomic and ionic deuterium efflux through formation of complex chemical bonds which sequester deuterium, making it unavailable for recycling [5,6].

Noteworthy improvements in plasma performance have followed from these lithium depositions on the graphite PFCs in NSTX, including a reduction and eventual elimination of the HeGDC time previously required between discharges, easier access to the H-mode, reduced edge neutral density, reduced plasma density particularly in the edge and SOL, increased pedestal electron and

\* Corresponding author.

E-mail address: [hkugel@pppl.gov](mailto:hkugel@pppl.gov) (H.W. Kugel).

ion temperature, improved energy confinement, and suppression of ELMs in the H-mode [1–4].

The NSTX results have hitherto depended on replenishment of the lithium coating on the PFCs between discharges by the LITERS. Without this replenishment, the beneficial effects of lithium disappeared within about 1–2 discharges. This can be understood, in part, from laboratory studies [5–7] which suggest that the retention of deuterium in lithiated graphite in the NSTX environment is less than implied by the stoichiometric formation of LiD due to (a) lithium intercalation in graphite, (b) lithium interactions with impurities in graphite, (c) lithium reactions with residual gases in the vacuum chamber, and (d) deuterium saturation of the lithium in the near-surface layers (<250 nm). Previous measurements of 20 keV deuterium incident on solid and liquid lithium found retentions approaching the stoichiometric limit for clean lithium, but lower for lithium with surface contamination [8,9]. Given the reactivity of liquid lithium with the residual gases in a typical vacuum chamber ( $H_2O$ ,  $CO$ ,  $CO_2$ ), achieving a fully absorbing lithium surface would require the use of flowing liquid lithium to remove impurities and refresh the surface. In 2010, as a prelude toward the design of possible flowing liquid lithium plasma facing surfaces, a Liquid Lithium Divertor (LLD) was installed in NSTX to test whether static liquid lithium would provide more deuterium retention, and for longer durations than the thin, solid lithium coatings on graphite previously investigated.

## 2. LLD design and installation

The LLD was installed in NSTX on the outer part of the lower divertor. Its design [10–12] encompassed the desired plasma requirements, the experimental capabilities and conditions, power handling, radial location, pumping capability, operating temperature, lithium filling, MHD forces, and diagnostics for control and characterization. The LLD operation goals included (a) achieving density control for improving the inductionless current drive capability (e.g., about a 15–25% density decrease from present high-performance discharges which often evolve toward the Greenwald density limit,  $n_e/n_{GW} \sim 1$ ), (b) producing a two-fold increase in  $n_e$  scan capability in the H-mode, (c) testing the ability to operate at significantly lower density (e.g.,  $n_e/n_{GW} = 0.25$ ), for future reactor designs based on the Spherical Tokamak, and (d) investigating high heat-flux power handling ( $10 \text{ MW/m}^2$ ) for long pulses ( $>1.5 \text{ s}$ ).

Shown in Fig. 1 is a schematic cross section of NSTX showing the location of the LLD and the LITERS. Fig. 2 shows a photo of the LLD installed on the outer part of the lower divertor prior to the start of operation in 2010. The LLD consists of four plates, 22 cm wide and each spanning  $80^\circ$  toroidally. The quadrants were separated toroidally by graphite tiles containing diagnostics and bias electrodes. The plasma-facing surface of the LLD has a 0.17 mm layer of molybdenum, plasma sprayed with 45% porosity onto a protective barrier of 0.25 mm stainless steel that is bonded to a copper substrate 2.2 cm thick. The molybdenum porosity is intended to facilitate wetting and subsequent spreading of liquid lithium over the LLD, and to make the lithium surface tension forces large relative to electromagnetic forces in the liquid layer, a function provided by metallic meshes and felts in previous experiments [13,14]. The lithium capacity of the porous surface was 37 g. Microscopic analysis of the molybdenum porosity indicates a scale length of about  $10 \mu\text{m}$  of which to first order yields a total lithium “wetable” area of about 8 times the geometric area of  $0.9 \text{ m}^2$ . The thin stainless steel serves as a barrier to prevent liquid lithium from reacting with the copper substrate to form a eutectic that could diffuse copper impurities to the plasma-facing surface. Each of the four LLD plates is supported at its corners to the divertor

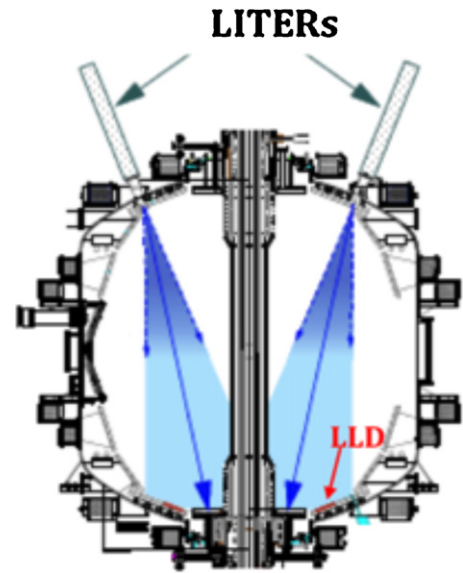


Fig. 1. Schematic cross section of NSTX showing location of the 2 Lithium Evaporators (LITERS) and the Liquid Lithium Divertor (LLD).

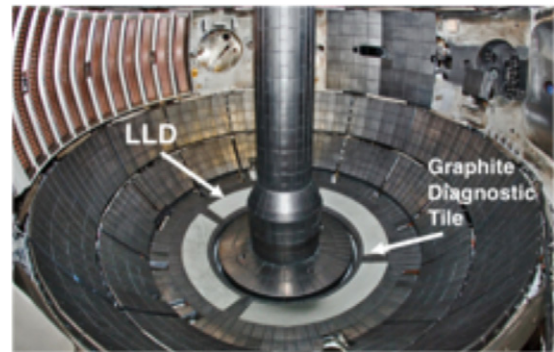


Fig. 2. Photo of the interior of NSTX before the start of the 2010 experimental campaign. Shown is the location of the Liquid Lithium Divertor (LLD) and the surrounding graphite tiles.

base-plate with fasteners providing electrical isolation, and allowing thermal expansion during vessel bakeout and plate heating during operation. A locating post positioned each LLD quadrant plate laterally relative to the divertor base-plates. The locating post engaged a hole in the bottom of the LLD plate. Copper “fingers” cladding this post provided single-point electrical grounding to the vacuum vessel. This post provided the primary path for currents following a disruption of plasma currents. Rogowski coils were mounted around each of the grounding posts to measure these currents.

Each of the four plates contained 12 embedded electrical resistive heaters (220 V, 400 W each), and 32 type-K thermocouples (Fig. 3). Prior to the failures discussed below, these electrical heaters

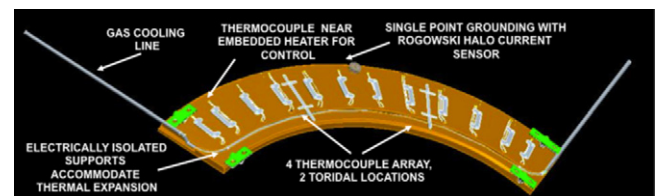


Fig. 3. Schematic of rear side (opposite plasma facing side) of one of 4 LLD plates showing the plate supports, single-point grounding, heaters, and instrumentation.

and also the embedded gas cooling lines (later also used to test heating with air) were used to maintain a surface temperature in the range 20–400 °C. The LLD heaters and the thermocouples were controlled by a dedicated computer. The control computer received timing signals from the facility clock to synchronize and remove power to the plate heaters while the NSTX applied fields were on. This prevented magnetic forces that might damage the plate heaters.

The electrical heaters of one of the LLD quadrants became inoperative at the outset of the campaign due to a failure in the wiring inside the vacuum vessel. Subsequently, after several months of operation, the heaters in two other quadrants failed, apparently as a result of a plasma current disruption. Following this second failure in the electrical heaters, the LLD plates were heated to temperatures of about 180 °C by passing compressed heated air through the cooling/heating lines embedded in the plates.

### 3. LLD 2010 operating procedure

The LLD was kept at room temperature overnight and during maintenance periods, and was only heated for specific experiments. The initial lithium depositions on the LLD with the LITER system were performed with three of the four LLD plates varied in bulk average temperature from ambient to 320 °C (the melting point of lithium is 180 °C). The fourth plate was only heated by the power flowing to the plate from the plasma which could produce an increase in its bulk temperature of about 10 °C for each typical 4 MW NBI discharge.

The LITER system was used to deposit lithium over the entire lower divertor region (spanning the major radius from 0.35 m to 1.1 m) which includes the graphite tiles and all four plates of the LLD (spanning the major radius from 0.65 m to 0.85 m). Initial deposition of 14 g of lithium was applied before plasma operation started, both to cover the porous molybdenum surface and to facilitate a rapid return to high-power H-mode plasmas. At the start of the 2010 experimental campaign, the accumulated lithium depositions on the LLD from LITER were a few grams (~5% of the 37 g capacity of its porous surface). At the end of the campaign, the total lithium deposited on the LLD surface exceeded 67 g, about twice its capacity. At that stage, for test purposes, LITER deposition was performed only at the start of each run day and was not applied between discharges.

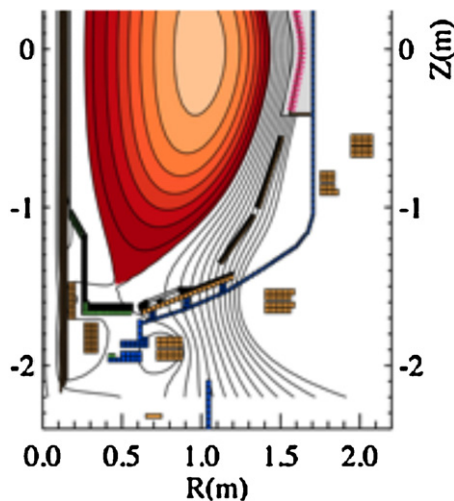


**Fig. 4.** Equilibrium fit to plasma shape used for high-elongation discharges with both strike points incident on lithiated graphite inboard of LLD which was located between major radius  $R=0.65$  m and  $R=0.85$  m.

## 4. LLD 2010 physics results

During the 2010 experimental campaign, lithium was evaporated over the entire lower divertor region (graphite tiles and LLD) for many different experiments employing plasma shapes ranging from high-elongation discharges with strike points inboard of the LLD to low-elongation discharges with their outer strike points directly on the LLD. Even for discharges without strike points on the LLD, power was incident on the LLD via the open field lines in the outer scrape-off layer. Four different LLD-specific experiments were performed as the total lithium deposited on the LLD increased.

Two methods were used to characterize the physics effects of the LLD. First, measuring the effects of the different lithium related edge response on the discharge characteristics, e.g., plasma edge temperature and density, plasma edge MHD stability (ELM-free H-modes), volume averaged density, stored energy, confinement time, etc. Second, measuring the amount of deuterium fuel gas needed to maintain similar reference discharges on graphite and the LLD, as lithium deposition was increased.

### 4.1. Effect of lithium related edge response on discharge characteristics

#### 4.1.1. LLD experiments at start of 2010 campaign

The initial experiments started with a thin lithium coating (~0.9 μm) on the lower divertor region. Using a standard lower single-null divertor discharge with its strike points inboard of the LLD, but with outer open field lines incident on the LLD with three plates heated to 319 °C, discharges were obtained that behaved similarly to plasmas on the lithium-coated graphite divertor prior to the installation of the LLD. Fig. 4 is a cross section of the plasma and Fig. 5 shows waveforms of this type of discharge which achieved quiescent, ELM-free, H-modes with 2 MW of NBI heating.

The initial 2010 LLD experiments, used discharges with the outer strike point on the LLD (Fig. 6), with the accumulated lithium deposition on the LLD in the range 1–10% of the porosity. The resulting plasmas were again typical of operating with lithium coated PFCs, i.e., ELM-free H-modes with low edge density, and improved confinement. The fueling required to maintain these discharges was about the same as discharges with the strike point inboard of the LLD.

#### 4.1.2. LLD experiments mid 2010 campaign

When the total lithium evaporated onto the PFCs had reached approximately 240 g, an experiment was conducted to investigate the effect of plasma heating of the surface with a series of discharges with 4 MW of NBI heating run with the outer strike point centered on the LLD, as shown in Fig. 6. At this stage, the porous LLD surface was estimated to be about 12% filled. Lithium continued to be evaporated between the discharges. During this series, a fueling scan was performed by deliberately increasing the deuterium gas fueling substantially. Fig. 7 shows the total number of deuterons added as gas and the resultant D and C<sup>6+</sup> plasma content at 0.5 s in each discharge. Also shown is the LLD surface temperature at 0.5 s which increased above the lithium melting point during the series. The difference between the deuterium gas input and the plasma deuterium content reached very high values in this experiment without disrupting the plasma, but there was little change the plasma deuterium content. This suggests that the added deuterium, after becoming ionized in the scrape-off layer flowed to the divertor and was absorbed by the liquid lithium rather than recycling and eventually increasing the plasma density.

About midway through the 2010 experimental campaign, a 75 h lithium evaporation was performed on the lower divertor area to yield a LLD lithium loading of about 50% of the capacity of its porosity. Then, discharges were run with the temperatures of the three

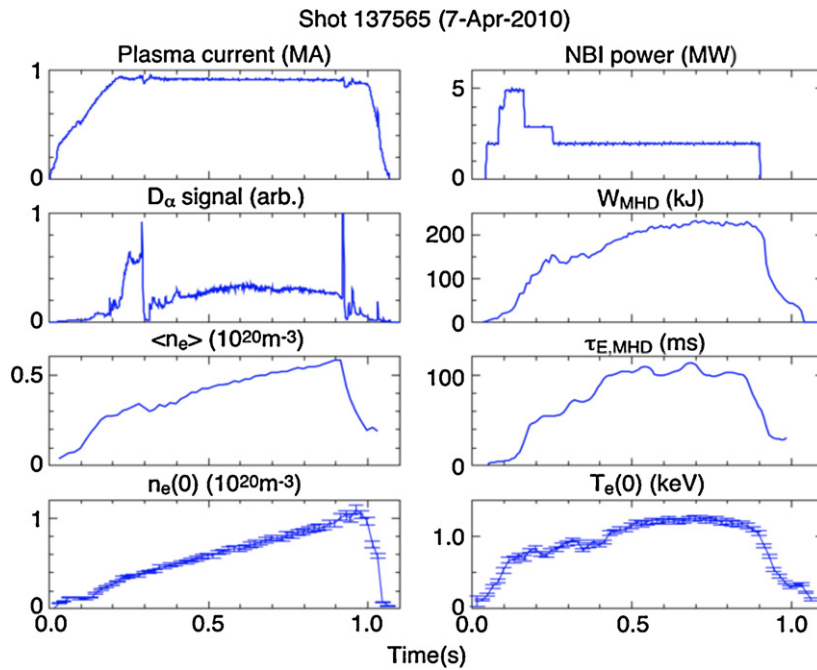


Fig. 5. Waveforms showing characteristics of high-elongation discharges with both strike points incident on lithiated graphite inboard of LLD.

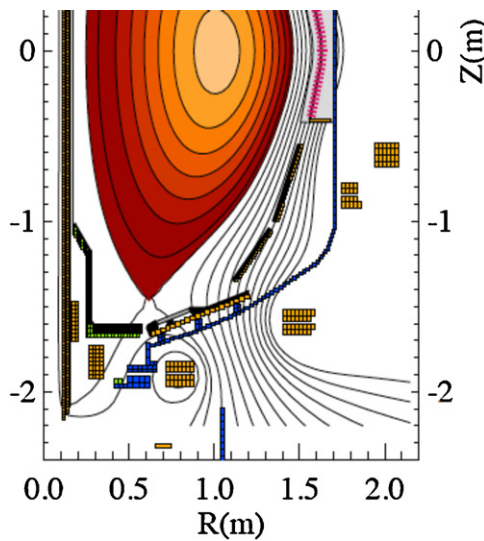


Fig. 6. Equilibrium fit to plasma shape used for low-elongation discharges with the outer strike point incident on the LLD and the inner strike point incident on lithiated graphite inboard of LLD.

electrically heated LLD plates varied from 50 °C to 300 °C. Similarly, in this experiment, operation with outer strike point on the LLD did not require more deuterium fueling. In addition, apparently due to the thickness of the coating, it was found that it was not necessary to use LITERS to replenish the lithium surfaces between discharges in order to maintain the desired lithium related edge response, *i.e.*, ELM-free H-modes, the low edge density, and improved confinement typical of operating with lithium coated PFCs. Deuteron plasma inventories were similar regardless of LLD temperature. Carbon inventories were similar to discharges run on the graphite PFCs coated with lithium. However, the divertor edge  $D_\alpha$  luminosity indicated a higher level of recycling from the divertor than had been observed earlier in the campaign. This was an indicator of changing nature of the LLD surface due to the integral effects of deuterium and impurity accumulation.

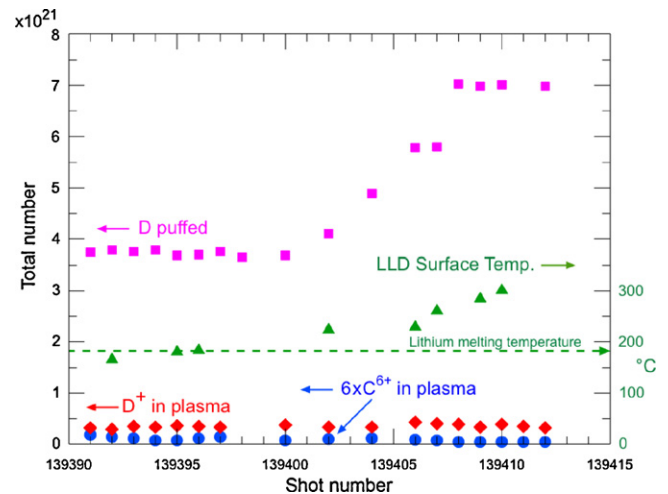


Fig. 7. Fueling scan data at 0.5 s for discharges with outer strike point on LLD. Shown is total number of deuterium particles puffed (gas fueling), and the resultant D and  $C^{6+}$  plasma content versus LLD surface temperature during the plasma.

#### 4.1.3. LLD experiments at end of 2010 campaign

At the end of the 2010 experimental campaign, as the accumulated lithium on the LLD surface exceeded more than 200% of its surface porosity capacity, experimental sequences were performed with either all LLD plates unheated, three plates heated (by hot air), or with all four plates heated by the heat efflux from diverted 4 MW NBI discharges with outer strike points on the LLD. In the last case, the plasma heating increased the LLD bulk temperature about 10 °C per discharge. The LLD average temperatures at the start of these discharges were in the range 57–102 °C. The peak LLD surface temperatures were measured during the discharge with a 2-color IR camera [15]. Since the measured LLD surface temperatures in the interval 500–600 ms reached 160–300 °C, the plasma at the outer strike point was incident on liquid lithium in many discharges. Fig. 8 shows that as the LLD plate surface temperature transitioned through the lithium melting point, the plasma electron and deuterium content remained relatively constant. Whereas

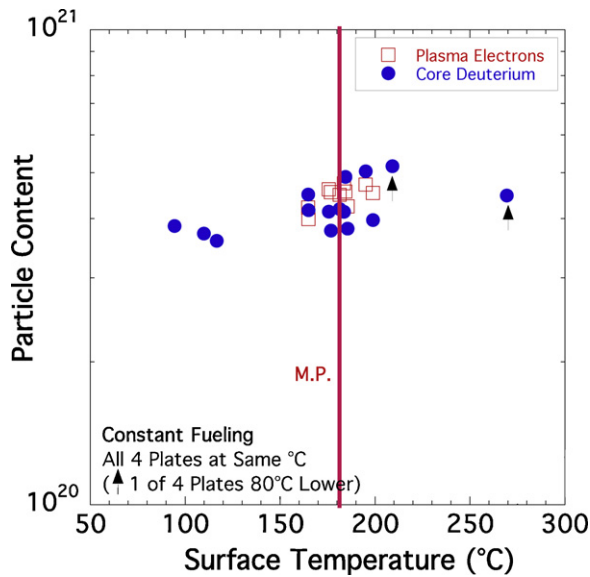


Fig. 8. Plasma D content measured using Charge Exchange Recombination Spectroscopy (CHERS) and the volume average plasma electron content versus LLD surface temperature during the plasma.

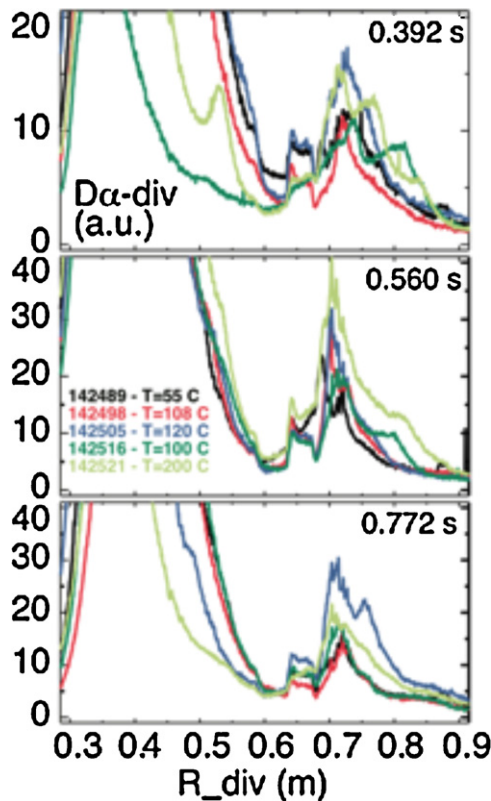


Fig. 9. D-alpha luminosity measured over the lower divertor from the inner strike point on liathed graphite ( $R=0.35$ ) to beyond the outer strike point on the LLD located between  $R=0.65$  m and  $R=0.85$  m.

the solid lithium coatings applied in 2008–2009 clearly suppressed the recycling flux, as indicated by the radial profile of the edge  $D_{\alpha}$  luminosity, it appeared that, under the LLD conditions for these measurements at the end of the 2010 experimental campaign, there was no systematic trend in the outer strike point divertor edge  $D_{\alpha}$  luminosity profile measured over the LLD as its temperature was increased by plasma heating (Fig. 9). Furthermore, the results of a global particle balance analysis [16,17] did not show systematic

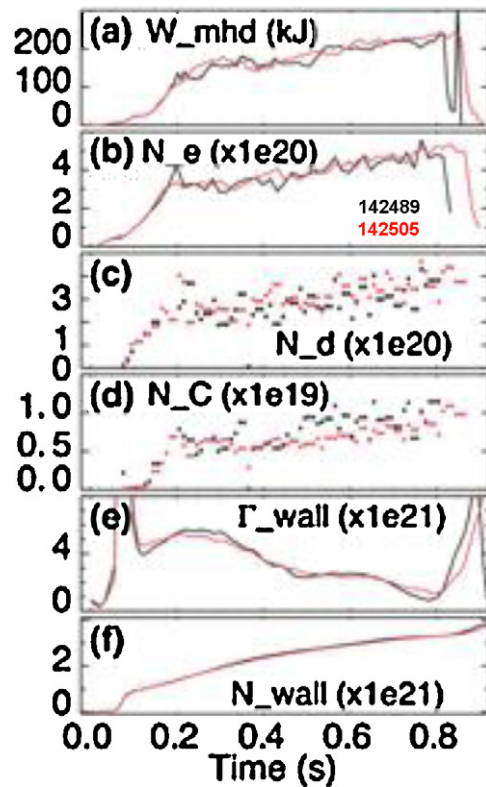


Fig. 10. The results of a global particle balance analysis for discharges with outer strike point on the LLD for a constant gas input when the LLD surface temperature was changed from 55 °C (black) to 199 °C (red). (For interpretation of the references to color in this figure legend, the reader is referred to the web version of the article.)

trends in the plasma or wall inventory (Fig. 10) for a constant gas input when the LLD surface temperature was changed from 55 °C to 199 °C,

### 5. LLD 2010 operating performance

#### 5.1. Operating performance during plasma discharges

During the 2010 experimental campaign, NSTX operated over 19.6 weeks and performed 3780 discharges. More than 50 experiments were performed involving diverted, NBI and RF-heated plasmas. Most of these experiments involved high-elongation plasmas with the diverted strike points incident on the inner graphite divertor inboard of the LLD. There were also more than 110 discharges with outer strike-points directly incident on the LLD. In addition, the LLD received small power and sputtering depositions from discharges not incident on the LLD, due to the open-field lines (beyond the last closed flux surface) incident on the LLD.

The thermal response of an LLD plate was dominated by its copper baseplate, but surface lithium was found to reduce the front face temperatures [15]. The analysis of lithium effects on the thermal response of the LLD (e.g., latent heat, and lithium radiation) are still under investigation. This demonstrated power-handling capability of the LLD for power depositions of  $\sim 5$  MW/m<sup>2</sup> for 1 s indicates that the plasma-sprayed bonding of the stainless steel barrier, and the diffusion bonding of the stainless steel to the copper baseplate performed successfully. No molybdenum line radiation from the plasma was observed, and inspection of the LLD surface after vessel venting yielded no visual evidence of power or cyclic thermal stress damage to the plasma sprayed porous molybdenum surface. These NSTX LLD results are consistent with the results of laboratory measurements of front face temperature measurements of an LLD



**Fig. 11.** Photo of the 2010 NSTX interior following 1.347 kg lithium deposition applied during 2010 experimental campaign indicates extensive lithium coverage due to direct evaporation and plasma transport. Shown is the white  $\text{Li}_2\text{CO}_3$  coating from conversion of Li and LiOH during air vent.

sample exposed to power densities of  $10 \text{ MW/m}^2$  for 1–3 s from a 30 keV neutral beam [18]. Optical micrographs with micron-level spatial resolution taken of the LLD sample before and after this beam exposure indicated no significant changes in surface morphology, other than what appeared to be some minor coalescence of the smallest particle sizes into larger particle sizes.

### 5.2. Inspection after vessel vent

After the 2010 experimental campaign, the vessel was vented with moist air for over 1 week before personnel entered the vessel for inspection. Shown in Fig. 11 is a photo of the NSTX interior following the total 1.347 kg lithium deposition applied during 2010 experimental campaign. The white coating on the entire interior is due to the conversion of residual elemental lithium into lithium hydroxide and finally inert lithium carbonate ( $\text{Li}_2\text{CO}_3$ ) during the air exposure. The extent of the white coating indicates the pervasive lithium coverage due to direct evaporation and plasma transport. Shown in Fig. 12 is a closer view of the lower divertor area and the LLD region. Dark features along most of LLD edges appear to be sputtered graphite from arcing between the LLD and the surrounding graphite tiles during plasma current disruptions (discussed below). Fig. 13 shows a closer view of these features.

The underside of the plates (opposite the plasma facing side) exhibited mechanical and electrical damage attributed to MHD forces during disruptions that exerted upward and radial outward forces on the plates. This damage consisted of (a) chipping and cracking of the adjacent graphite tiles and abrasion of the heating/cooling tubes caused by rotation of the plates about their locating posts (b) damage to the plate corner supports including three broken support screw pins, deformed copper support holes, and arcing to surrounding structure, and (c) damage to the electri-



**Fig. 12.** View of lower divertor region showing LLD and surrounding graphite tiles. The dark regions at the edges of the LLD plates exhibit sputtered graphite deposition due to arcing.

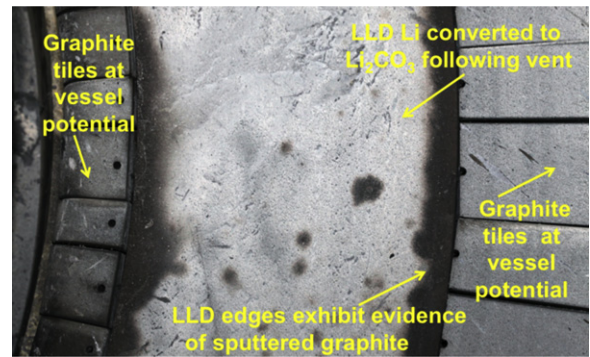


**Fig. 13.** The blackened LLD edges exhibit evidence of sputtered graphite from arcing between the plate and graphite tile at vessel-ground potential.

cal ground post by arcing. Each stainless steel grounding post on the outer side of the LLD was surrounded by copper finger-stock (electrical joint expandable copper straps) to facilitate electrical conduction from the plate to vessel ground. The post-vent inspection found that these copper “fingers” were melted, presumably due to plasma linked wall currents during plasma current disruptions. Arcing damaged was also exhibited by insulation failure and damage to the gas cooling/heating lines about 1 cm outboard of the LLD.

During LLD testing, prior to the start of plasma operations, the heater cable bundle from one of the quadrant plates failed. Post-vent inspection found that this cable bundle experienced an insulation failure inside the vessel and short circuited the cables to vessel ground. Later in the campaign, air heating of all four quadrant plates via the bottom-side cooling tube (Fig. 3) was tested successfully. During an LLD heating experiment, one of the external resistive air heating units failed.

### 5.3. Cleaning and repair of the LLD following the experimental campaign

After each annual experimental campaign, before the NSTX vessel is entered for maintenance, the vessel is vented for at least one week using moist air to render inactive (passivate) any residual active lithium or lithium hydroxide. This process converts active lithium and lithium compounds to inert lithium carbonate ( $\text{Li}_2\text{CO}_3$ ), which is then removed by washing the surface with a 5% solution of acetic acid (common vinegar). This converts the insoluble  $\text{Li}_2\text{CO}_3$  into water-soluble lithium acetate, which is easily removable by rinsing with water.

After the 2010 vent, the LLD plates were removed from the vessel for maintenance and cleaning. Shown in Fig. 14 is a test cleaning of a section of a plate which illustrates the prompt action (20 min) of vinegar in removing  $\text{Li}_2\text{CO}_3$ . The residual stains shown in Fig. 14 appear to be due to residual micron-size graphite particles deep in the porous molybdenum. This material could possibly be removed by soaking the plate in an ultrasonic bath of commercial detergent, such as is used for cleaning vacuum components. However, this was not done due to uncertainties about the effect of ultrasonic vibration deteriorating the mechanical bonding of the plasma-sprayed molybdenum to its stainless steel substrate. In addition, the commercial detergents normally used for cleaning vacuum components in ultrasonic baths typically contain sodium compounds that could remain in the porous molybdenum and contaminate the plasma if not completely removed during the cleaning process. After the cleaning process was completed, some regions of the residual graphite stains exhibited a slight bluish tinge, indicative of molybdenum oxides [19].

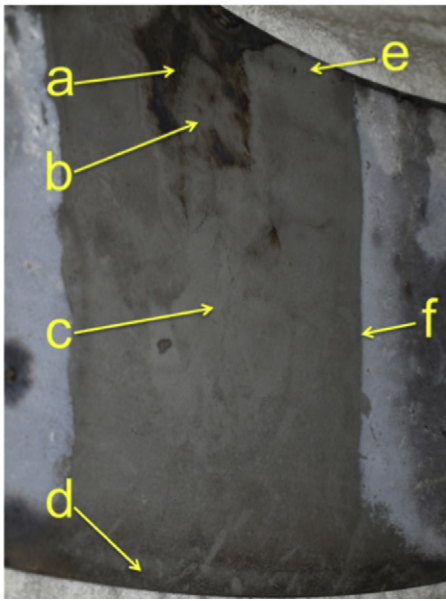


**Fig. 14.** Photo of LLD plate partial cleaning test by flowing re-circulating vinegar over  $10^\circ$  sloping surface for 20 min using a peristaltic pump: (a) dark discoloration appeared to be slowly dissolving with additional soaking, (b) small red-brown patch found under original top layer had appearance of lithium nitride ( $\text{Li}_3\text{N}$ ) and dissolved-off, (c) original thick coarse  $\text{Li}_2\text{CO}_3$  coating dissolved-off, (d) carbon-like black region along outboard rim peeled-off, (e) carbon-like black region along inboard rim peeled-off, and (f) edge of cleaning test. The residual dark stains appeared to be micron-size graphite embedded in the molybdenum pores. (For interpretation of the references to color in this figure legend, the reader is referred to the web version of the article.)

## 6. Discussion

### 6.1. Discussion of LLD 2010 physics results

The NSTX LLD 2010 results exhibit similarities to the earlier experiments where lithiated graphite covered the entire lower divertor, including the region presently occupied by the LLD. During the 2010 LLD experiments, the deuterium fueling needed to maintain stable, 1 s long reference discharges with the outer strike point on the LLD, was the about the same as that for lithium coated graphite prior to the installation of the LLD, *i.e.*, about two times that of no-lithium conditions. Using this required discharge fueling as an indicator of the degree of deuterium retention implies that deuterium retention in the lithiated graphite and liquid lithium in the LLD were comparable for these discharges. In addition, similar discharge edge improvements were obtained (*e.g.*, quiescent edge, ELM-free, H-modes).

These results suggest that the deuterium incident on lithiated graphite and on the liquid lithium of the LLD was being retained with comparable efficiency. Laboratory measurements of 20 keV deuterium incident on solid and liquid lithium have previously found deuterium retentions approaching the stoichiometric amount for formation of  $\text{LiD}$  for clean lithium, but lower levels for lithium with surface contamination [8,9]. The present results for solid and liquid lithium, do not determine the degree of deuterium retention, or the nature of the retention in the respective lithiated surfaces under NSTX conditions because lithium coated graphite was always present in addition to the lithium coated LLD. Thus, we have not determined at this time whether the solid lithium and liquid lithium retention factors are near unity, or are both much less than unity, but due to different mechanisms. For example, the retention of deuterium efflux in lithium-coated graphite in the NSTX environment might be less than unity due to lithium intercalation in graphite [7], lithium interactions with impurity complexes

in graphite [5,6], and deuterium saturation of the lithium surface layers (the range of thermal  $\text{D}^+$  in lithium is  $<250$  nm) [20]. Similarly, the reactivity of deuterium incident on liquid lithium could be less than unity due surface impurity complexes inhibiting lithium deuteride formation, or the possibility that incident deuterium reaction products do not diffuse away from the surface at a rate faster than the rate of formation, thereby effectively establishing a saturated layer. This could occur also if impurities accumulate in the near surface layer [21]. Additional laboratory and NSTX work is in progress to resolve these questions.

### 6.2. Discussion of LLD 2010 operating performance

In-vessel inspection of the LLD following the 2010 experimental campaign found mechanical damage to the LLD plate supports and other hardware, indicating that this damage resulted from vertical and radial forces following plasma current disruptions. The initial design considered the effects of electromagnetic forces due to eddy currents from rapid flux changes in the plates due to collapsing magnetic fields during a plasma current disruption, and plasma edge currents flowing through the plates as the plates become enveloped in plasma during the plasma current decay. The estimated maximum impulsive load due to this effect was about  $4.3 \times 10^3$  N on the radial edges of the plate and about  $2.3 \times 10^3$  N on the toroidal edges. The forces on the LLD curved edges tend to push it outward toward larger major radii while the forces on the ends tend to twist the plate about a radial axis. The result is that the corner supports resist vertical forces; the centering post resists radial forces. Failure of the plate electrical isolation at the corners would allow additional induced current loops and could increase these forces by a factor of about 4. The Rogowski coils on the center ground posts of the LLD plates showed a decrease in the measured ground current as the experimental campaign progressed. However, the currents measured in instrumented graphite tiles outboard of the LLD did not show a similar decrease in currents measured during disruptions. This behavior is consistent with additional electrical contacts from the LLD plates to the divertor floor developing later in campaign providing alternate current paths and the possible formation of large-area conducting loops intercepting poloidal flux.

## 7. LLD 2011 operation and planned experiments

The LLD plates were removed from the vessel for maintenance at the end of the 2010 campaign. All of the original heaters, thermocouples, and cooling/heating tubes were removed from the plates. The plates were refurbished with stronger corner support design to resist rotation and lifting forces. Threaded corner fasteners connecting the corner supports to the copper baseplate were replaced by a locking ring design. The insulation of the corner supports was improved. Two alignment plugs were installed and positioned to stop rotation. The copper finger-stock of the original electrical grounding design was replaced by a thick copper braid and fastening lug. The original 36 thermocouples in each plate were replaced with three new type-K thermocouples. The removed electrical heating units were not reinstalled. Hence, only plasma heating will be available for experiments in 2011.

In addition, to these changes to the LLD, the first row of graphite tiles on inboard divertor next to the LLD have been replaced by molybdenum tiles (TZM alloy). These include three sensor tiles containing respectively a type-K thermocouple, a Langmuir probe, and a 2D-Mirnov coil. This configuration will allow both the inner and outer strike points to be positioned on lithiated molybdenum to test whether this reduces the sputtering of carbon from the divertor, and will allow characterization of lithiated, metal divertor surfaces.

## 8. Summary and conclusion

In 2010 NSTX installed a Liquid Lithium Divertor (LLD) to test if static liquid lithium would provide increased deuterium retention, and for longer durations than thin, solid lithium on graphite. In terms of the deuterium fueling needed to maintain similar reference discharges, there was no significant difference between discharges with the divertor strike point on graphite or the unheated LLD, as lithium deposition was increased. Thus, the effective LLD pumping of deuterium was the about the same as that for solid lithium coatings on graphite, *i.e.*, about twice that of no-lithium conditions. Other indications of plasma performance, including the H-mode power threshold, the suppression of ELMs by lithium, the confinement and the plasma stability appeared to be unaffected by the LLD. No molybdenum line radiation was observed in the plasma.

In one experiment, deliberately adding a relatively large amount of deuterium fuel to discharges with the outer strike point on the LLD did not change the plasma deuterium content and did not destabilize the plasma. This may indicate that the additional deuterium fuel gas became ionized in the scrape-off layer, flowed to the divertor and was absorbed by the liquid lithium before it could increase the plasma density. This observation, however, was not definitive because the experiment of cooling the LLD to the lithium solidification temperature to allow the solid lithium to saturate and restore deuterium recycling was not performed. Additional work is planned to resolve this question.

Inspection of the LLD after vessel venting yielded no evidence of power damage or cyclic thermal stress damage to the plasma sprayed porous molybdenum LLD surface. However, there was mechanical and electrical damage on the underside of the plates apparently produced by disruptions.

The LLD plates have now been refurbished and reinstalled. A row of molybdenum tiles has been installed inboard of the LLD to

allow experiments with both inner and outer strike points on lithiated molybdenum. This capability will allow further investigation of some of the lithium PFC issues encountered in the first testing of the LLD.

## Acknowledgements

This work supported by USDOE contracts DE-AC02-09CH11466 (PPPL), DE-AC05-00OR22725 (ORNL), and DE-AC52-07NA27344 (LLNL).

## References

- [1] H.W. Kugel, et al., *Phys. Plasmas* 15 (2008) 056118.
- [2] H.W. Kugel, et al., *J. Nucl. Mater.* 390–391 (2009) 1000.
- [3] M.G. Bell, et al., *Plasma Phys. Control. Fusion* 51 (2009) 124056.
- [4] H.W. Kugel, et al., *Proc. 19th PSI, San Diego, CA, May 24–28, 2010, J. Nucl. Mater.*, in press, doi:10.1016/j.jnucmat.2010.12.016.
- [5] J.P. Allain, et al., *J. Nucl. Mater.* 390–391 (2009) 942.
- [6] C.N. Taylor, et al., *Proc. 19th PSI, San Diego, CA, May 24–28, 2010, J. Nucl. Mater.*, in press, doi:10.1016/j.jnucmat.2010.9.049.
- [7] N. Itou, et al., *J. Nucl. Mater.* 290–293 (2001) 281.
- [8] S.K. Erents, G.M. McCracken, P. Goldsmith, *J. Phys. D: Appl. Phys.* 4 (1971) 672.
- [9] A.K. Fischer, D.V. Steidl, Brient, *Nucl. Sci. Eng.* 63 (1977) 191.
- [10] H.W. Kugel, et al., *Fusion Eng. Des.* 84 (2009) 1125.
- [11] R.E. Nygren, et al., *Fusion Eng. Des.* 84 (2009) 1438.
- [12] R. Ellis, et al., *IEEE/NPSS 23rd Symposium on Fusion Engineering*, San Diego, CA, June 1–5, 2009, 2009, ISBN 978-1-4244-2635-5, p. 1.
- [13] V.A. Evtikhin, et al., *Plasma Phys. Control. Fusion* 44 (2002) 955.
- [14] S.V. Mirnov, et al., *J. Nucl. Mater.* 390–391 (2009) 876.
- [15] A. McLean, *Proc. 2nd Int. Symposium on lithium Applications for Fusion Devices*, Princeton, New Jersey, USA, April 27–29, 2011.
- [16] V.A. Soukhanovskii, et al., *Nucl. Mater.* 313–316 (2003) 573.
- [17] V.A. Soukhanovskii, et al., *Proc. 23rd Int. Conf. Fusion Energy*, Daejeon, Korea, 2010.
- [18] T. Abrams, *Proc 2nd Int. Symposium on lithium Applications for Fusion Devices*, April 27–29, Princeton, New Jersey, USA, 2011.
- [19] J.R. Arthur, *Nature* 164 (1949) 537.
- [20] J.N. Brooks, et al., *J. Nucl. Mater.* 337–339 (2005) 1053.
- [21] R. Bastz, J.A. Whaley, *Fusion Eng. Des.* 72 (2004) 111.